Journal of Power Sources 196 (2011) 9036–9045

Contents lists available at ScienceDirect

Journal of Power Sources

journal homepage: www.elsevier.com/locate/jpowsour

Model-based development of low-level control strategies for transient operation of solid oxide fuel cell systems

Marco Sorrentino*, Cesare Pianese

Department of Mechanical Engineering – University of Salerno, Via Ponte Don Melillo, 84084 Fisciano (SA), Italy

ARTICLE INFO

Article history:
Received 3 November 2010
Received in revised form 6 January 2011
Accepted 7 January 2011
Available online 19 January 2011

Keywords:
Solid oxide fuel cells
SOFC systems
Fuel cell dynamics
Cold-start
Low-level control

ABSTRACT

The exploitation of an SOFC-system model to define and test control and energy management strategies is presented. Such a work is motivated by the increasing interest paid to SOFC technology by industries and governments due to its highly appealing potentialities in terms of energy savings, fuel flexibility, cogeneration, low-pollution and low-noise operation.

The core part of the model is the SOFC stack, surrounded by a number of auxiliary devices, i.e. air compressor, regulating pressure valves, heat exchangers, pre-reformer and post-burner. Due to the slow thermal dynamics of SOFCs, a set of three lumped-capacity models describes the dynamic response of fuel cell and heat exchangers to any operation change.

The dynamic model was used to develop low-level control strategies aimed at guaranteeing targeted performance while keeping stack temperature derivative within safe limits to reduce stack degradation due to thermal stresses. Control strategies for both cold-start and warmed-up operations were implemented by combining feedforward and feedback approaches. Particularly, the main cold-start control action relies on the precise regulation of methane flow towards anode and post-burner via by-pass valves; this strategy is combined with a cathode air-flow adjustment to have a tight control of both stack temperature gradient and warm-up time. Results are presented to show the potentialities of the proposed model-based approach to: (i) serve as a support to control strategies development and (ii) solve the trade-off between fast SOFC cold-start and avoidance of thermal-stress caused damages.

© 2011 Elsevier B.V. All rights reserved.

1. Introduction

In the last years, solid oxide fuel cells had gathered a large attention mainly for their potential application as stationary power generators and APUs for transportation use (ground, marine, air). The primary reason for their attractiveness lies on both the high energy conversion efficiency and the zero toxic emission levels (only the CO_2 released by the hydrogen production process is a concern). Other advantages are: modularity, fuel flexibility and low noise [1–3]. Moreover, the high working temperatures provide additional positive features, such as potential use of SOFC in highly efficient cogeneration applications [3]. SOFCs also are suitable for internally reforming the fuel (e.g. natural gas, propane, methanol, gasoline, diesel, etc.), thus avoiding the adoption of highly sophisticated and expensive external reformer and simplifying fuel storage also [2]. Nevertheless, the big challenges to promote SOFC systems diffusion are mainly related to production costs and durability. Among others, European (Fuel Cell and Hydrogen Joint Technology Initiative – NEW IG) [4], American (Solid State and Energy Conversion Alliance – SECA) [1] and Japanese (New Energy and Industrial Technology Development Organization – NEDO) [5] organizations are following independent research programs to pursue the mentioned objectives. The achievement of these targets will surely contribute to promoting the technology and finally starting a mass production phase. Once this goal is reached, potential areas of application in the short term will be small residential power generators and vehicles' APUs. In the long term scenario, SOFC applications could be reasonably extended to marine, rail and airplane APUs, high-power stationary generators and even to marine and rail propulsion [6].

To support the successful deployment of SOFC, specific computational tools to support stack and balance of plant sizing, as well as control and diagnostics strategies design are required to simulate both steady and transient conditions. Steady-state models serve at important aims, such as improving knowledge of internal processes occurring inside the SOFC, individuating the optimal operating set-points and determining stack size as function of nominal power demand. On the other hand, modeling SOFC dynamics is a key requirement for even more critical aspects. Prediction of SOFC response to load change allows evaluating the thermal stresses imposed to cell components during transients. Therefore, selection of materials, components design and control strategies definition

* Corresponding author. Tel.: +39 089964081; fax: +39 089964037.
E-mail address: msorrentino@unisa.it (M. Sorrentino).

0378-7753/$ – see front matter © 2011 Elsevier B.V. All rights reserved.
doi:10.1016/j.jpowsour.2011.01.023

Nomenclature

Acronyms

CS	cold start
SOFC	solid oxide fuel cells
WU	warmed up

Roman symbols

A	electroactive area (m^2)
A_{HE}	air pre-heater heat transfer area (m^2)
C	fluid heat capacity ($J\,K^{-1}$)
c_p	specific heat at constant pressure ($J\,kg^{-1}\,K^{-1}$)
$\dot{E}$	energy rate (W)
I	current (A)
J	current density ($A\,cm^{-2}$)
K	heat capacity ($J\,K^{-1}$)
$\dot{m}$	compressor air flow ($kg\,s^{-1}$)
$\dot{m}_{air,in,cs-wu}$	air flow to the cathode at the beginning of the transition CS–WU ($kg\,s^{-1}$)
$\dot{m}_{CH_4,cs}$	cold start methane flow ($kg\,s^{-1}$)
P_{cp}	compressor power (kW)
P_{gross}	gross SOFC power (kW)
P_{net}	net SOFC power (kW)
t	time (s)
T	temperature (K)
U	lumped heat transfer coefficient ($W\,m^{-2}\,K^{-1}$)
U_f	fuel utilization
V_i	ith valve
V_{SOFC}	SOFC stack voltage (V)

Greek symbols

β	compression ratio
η_{cp}	compressor efficiency
η_{EM}	compressor drive motor efficiency
λ	excess of air fed to the SOFC

Subscripts

0	initial state
a	ambient air
c	cold fluid
cat	cathode
des	desired
f	final state
h	hot fluid
HE	air pre-heater
in	inlet
out	outlet
pb	post-burner
req	required

are enhanced. Moreover, definition of both optimal control and diagnostics strategies entails implementing computational tools that meet the conflicting needs of accuracy, affordable computational time, limited experimental efforts and flexibility. Therefore the development of a class of models complying with the above requirements is crucial towards the achievement of reliable on-field monitoring, control and diagnostics strategies [24].

Regarding stack durability, it is well known that actual SOFC system prototypes suffer from a low reliability of both the fuel cell itself and the complete system, not allowing a commercial deployment of such systems yet. At the actual stage, system state of health can hardly be evaluated, making it difficult to handle faults or degradation with an appropriate counter measure. This is the reason why cooperative work on SOFC modeling, control and diagnostics is now strongly encouraged by research organizations, such as the European research organization N.ERGHY [7]. In order to optimize the control actions and degradation prevention capabilities, specific diagnostic methods are needed to determine the actual state of the stacks in real-time. Once fast and reliable diagnostics will be available, adaptive control strategies, able to modify the control laws on-board, will be introduced. Due to their intrinsic features, adaptive control algorithms require dynamic models to be developed. Therefore fast and accurate SOFC dynamic models represent a key point towards the implementation of advanced control strategies able to guarantee both optimal performance and lifetime enhancement.

The availability of steady-state models, ranging from 3-D, CFD-solver based to 0-D (i.e. lumped) approaches, is considerable, as documented by the high number of publications focusing on such topic [3,8–10]. On the other hand, the number of publications devoted to SOFC dynamic modeling is lower (although increasing in the last years), thus clearly indicating that the field requires significant contribution yet. Indeed, most dynamics models currently available on the public domain [11–13] were developed following physical (i.e. 1-, 2- or even 3-D) approaches, which certainly ensure accurate prediction of SOFC performance but, on the other hand, may result in undesirably high computational intensity. This is in contrast with the requirements of SOFC manufacturers and developers. Furthermore, the definition of the optimal control strategies for SOFC power units, as it is for the majority of engineering applications, can be hardly pursued without recurring to less computational intensive models. To this purpose, interesting lumped approaches were followed in [14] and for control of SOFC-based distributed generators [15].

Some contributions are available concerning modeling, sizing and control of the SOFC stack and its ancillaries. In contribution [16] a model was proposed to describe thermal and mass transfer dynamics inside a hydrogen-fed standalone SOFC-APU with assigned specifications. The paper [17] deals with the development of a simplified dynamic model for an automotive hydrogen-fed SOFC-APU assisted by the thermal engine during the heat-up phase. Previous works conducted by the authors have already addressed these topics focusing on different modeling approaches [18,19]. An example of SOFC-APU BoP sizing was presented recently [20], proving the potentialities of models integration for SOFC control design applications. Moreover, the same computational structure was also shown to be suitable for on-board diagnostics strategies development [21].

In the following sections a description of the proposed grey-box modeling together with the motivation of this approach is given. Then the use of the model for developing low-level control strategies, which are suitable for ensuring efficient as well as safe operation of SOFC systems in both cold-start and regime operations, is presented. These strategies have been developed with the objective to solve the trade-off between low stack gradient temperature and warm-up time, which in turn is related to stack temperature time-derivative. Since the control actions should be able to cope with system management problems (e.g. load, heat management), a fast actuation is required. With reference to either warm-up or warmed-up conditions the air has to be considered as stack heating or cooling fluid, respectively; on the other hand the fuel is a chemical energy carrier whose conversion generates heat from either combustion in the post-burner or electrochemical reaction in the stack. Therefore, a combination of feedforward and feedback actions is implemented to control air and fuel streams. In the proposed configuration, during cold start an anode by-pass circuit splits the methane flow between pre-reformer/stack and post-burner (see Fig. 2). This allows controlling the temperature of both anode inlet gases and post-burner outlet stream, which is used in the pre-heater to heat up the air flowing into the cathode; therefore a tight control of the stack temperature is achieved. On

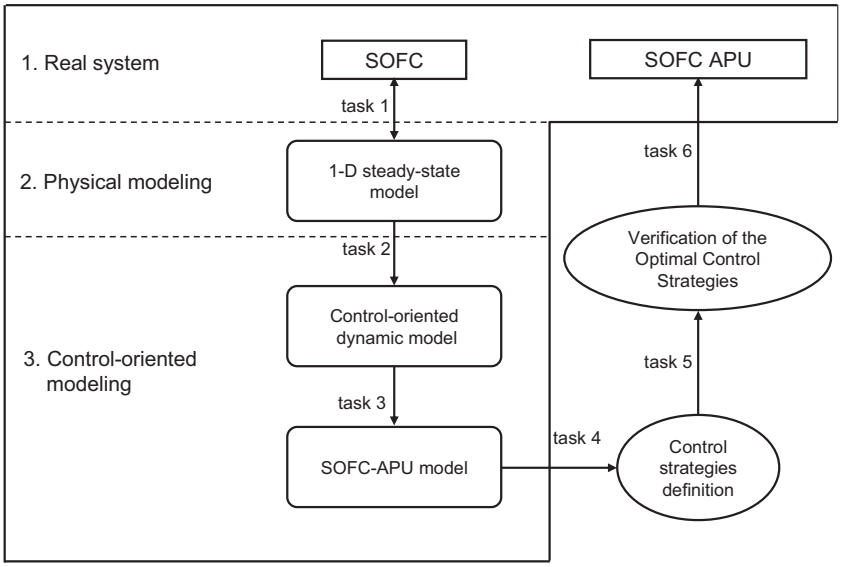

Fig. 1. Hierarchical approach for modeling (tasks 1, 2), simulation (task 3), control strategies definition (tasks 4, 5) and implementation (task 6) of an SOFC-APU.

the other hand at warmed-up a simpler control strategy is adopted for the fuel feeding.

2. Model-based approach to control strategies definition in SOFC systems

SOFC control design requires the use of specific models to guarantee reliable strategies to achieve control targets, which must be attained through safe stack states sequences. The most critical issue, which strongly constraints the choice of the operating path (the shortest and/or the most efficient), is the avoidance of high thermal derivatives both in space and time domains that may be experienced by the stack materials under transient operations. Therefore, dynamic analyses are required to develop and optimize control strategies. On the other hand, the attainment of a comprehensive database, including transient experimental data, is strongly limited by the enhancement of stack degradation during load cycles or gas feeding transients, which in turn may cause either performance losses or stack failure. Therefore several stacks should be used to have an exhaustive mapping, which results in high testing costs and long time; furthermore a loss in statistical significance of the measured data may also occur. From the brief considerations reported, the use of dynamic models to support the control design process is mandatory and a proper selection of the modeling approach must be performed to guarantee the required accuracy. Moreover, the models should not rely on large experimental data set for their development.

Modeling approaches may vary depending upon the specific application field. Obviously, models with high physical content are required to improve component design. As mentioned in the previous section, for system sizing and optimal-control strategies definition black-box and grey-box models are both more suitable than physical, high computational intensive models. Furthermore, control strategy optimization can be achieved adopting large-scale design optimization algorithms, which usually require several function evaluations [22]. Therefore, the use of models with a good compromise between accuracy and computational time must be considered.

Optimal control strategies are defined at both supervisory (i.e. high control level) and low control level [23]. The definition of the optimal working set-points, which competes to higher control levels, does not necessarily require dynamic simulations. On the other hand, low-level controls are often accomplished via feedback strategies, thus requiring taking into account the main system dynamics. In both cases, optimization analyses have to be performed, thus suggesting the combined use of steady and dynamic grey/black-box models.

It is reasonable to expect that physical models demand for relatively few experimental data for their validation. On the other hand, black-box approaches entail performing a high number of experiments to be used for both identification and test. On the basis of the previous discussion the use of large set of dynamic experiment is the main drawback in applying model-based design methodologies for control design of SOFC systems. Therefore, experimental burden has to be accounted for as a further conflicting need in the trade-off analysis on modeling approach. Such issue can be addressed by recurring to a hierarchical approach. Particularly, the use of physical models can be optimized, in that once tested for validation with a reduced amount of experimental data, they can be used as virtual-experiments generators. In such a way, the available reference data sets can be extended and then, following the hierarchical sequence shown in Fig. 1, black-box models can be identified and validated without further impact on experimental burden.

2.1. SOFC system: modeling approach

Nowadays, engineering research is always based on the mathematical representation of the physical system under-investigation. Modeling approaches may vary depending upon the specific application field. As expected, high physical description is required for models devoted to improve component design, while for system sizing, optimal-control strategies definition and diagnostics algorithms' development, black-box and grey-box models are well suited. Indeed, these latter approaches are more appropriate than physical-based ones when intensive model use is required such as the cases that involve high function evaluations. Some examples refer to (i) optimal balance of plant, which may be achieved adopting large-scale design optimization algorithms [22]; (ii) transient simulations for thermal stack response analysis with respect to control actions; (iii) degradation studies, to be performed by combining fast models with a statistical representation of both operative and state variables.

In the following a grey-box model applicable to the previous cases is presented. Further details can be retrieved from previous papers [19,20]. Fig. 2 provides a schematic representation of an SOFC system whose sizing is described in [21]. It is worth men-

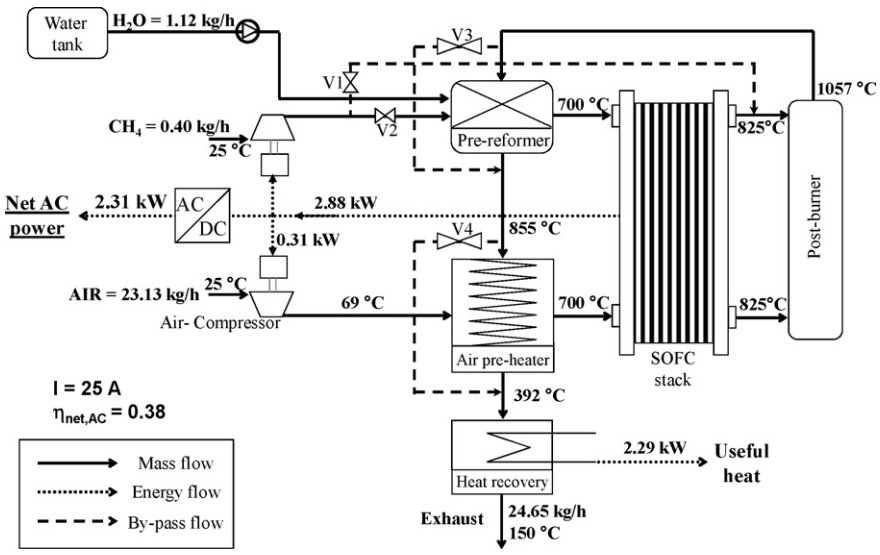

Fig. 2. Plant schematic of an APU consisting of 150 SOFCs with description of energy and mass flows at the nominal operating point (i.e. $I = 25$ A, i.e. $J = 0.25\ \mathrm{A\,cm^{-2}}$). Further details on system specifications can be retrieved from [20].

tioning that operating data reported in Fig. 2 refer to the most efficient operating condition, whereas maximum power (i.e. 5 kW) is reached at current density as high as $0.8\ \mathrm{A\,cm^{-2}}$. Fuel utilization is constantly set to 70%.

2.2. SOFC stack

For the purpose of the present application the SOFC stack can be treated as a control volume exchanging mass and energy with its surroundings. Under the hypothesis listed below, the lumped capacity model expressed by Eq. (1) is obtained by applying the first thermodynamic principle to a planar co-flow SOFC fed by reformate methane:

- Spatial variations are not considered, i.e. lumped modeling approach.
- Adiabatic components.
- Water gas shift reaction is considered at equilibrium.
- Mass transfer and electrochemistry are assumed instantaneous.

$$K_{\mathrm{SOFC}}\frac{dT_{\mathrm{SOFC,out}}}{dt} = \dot{E}_{\mathrm{SOFC,in}}(T_{\mathrm{SOFC,in}}) - \dot{E}_{\mathrm{SOFC,out}}(T_{\mathrm{SOFC,out}}) - J\cdot A\cdot V_{\mathrm{SOFC}} \tag{1}$$

where $\dot{E}_{\mathrm{SOFC,in}}$ and $\dot{E}_{\mathrm{SOFC,out}}$ are the energy flows in and out of the stack, respectively, and V_{SOFC} is the SOFC voltage evaluated through the following black-box regression type model [19]:

$$V_{\mathrm{SOFC}} = 27.66 - 12.28\cdot U_{\mathrm{f}} - 185.28\cdot J + 0.6204\cdot\lambda\cdot\frac{T_{\mathrm{SOFC,out}}}{1000} + 128.91\cdot J\cdot\frac{T_{\mathrm{SOFC,out}}}{1000} + 107.3\cdot\frac{T_{\mathrm{SOFC,in}}}{1000} \tag{2}$$

2.3. Air compressor

The parasitic power required by the air compressor, which serves at supplying the total amount of air needed to meet both electroxidation reaction and stack cooling requirements, is modeled as follows:

$$P_{\mathrm{cp}} = \dot{m}\frac{c_{\mathrm{p}}T_{\mathrm{a}}}{\eta_{\mathrm{EM}}\cdot\eta_{\mathrm{cp}}}\left[\beta^{(k-1)/k} - 1\right] \tag{3}$$

where the efficiency terms are evaluated as function of operating condition through suited look-up table, either provided by the manufacturer or experimentally identified [20]. Since P_{cp} can be considered as the main parasitic loss due to ancillaries functioning, the following approximations can be safely introduced for gross and net power delivered by SOFC stack and SOFC system, respectively:

$$P_{\mathrm{gross}} = V\cdot J\cdot A \tag{4}$$

$$P_{\mathrm{net}} = P_{\mathrm{gross}} - P_{\mathrm{cp}} \tag{5}$$

2.4. Post-burner

Main aim of this sub-model is to evaluate exit post-burner temperature ($T_{\mathrm{pb,out}}$) after combustion of residual H_2 and CO molecules held by the anodic exhaust stream. Particularly $T_{\mathrm{pb,out}}$ is estimated solving the following energy balance, under the assumption of complete adiabatic combustion of residual H_2 and CO [20,25]:

$$\dot{E}_{\mathrm{pb,in}}(T_{\mathrm{SOFC,out}}) = \dot{E}_{\mathrm{pb,out}}(T_{\mathrm{pb,out}}) \tag{6}$$

2.5. Air pre-heater and pre-reformer

Zero-Capacity-Approach (ZCA [26]) was followed to model heat exchange occurring in the air pre-heater. Particularly, dynamic variation of hot and cold fluid temperatures is modeled as follows:

$$\text{hot fluid}: \quad (K_{\mathrm{HE}} + C_{\mathrm{h}})\frac{dT_{\mathrm{h,HE}}}{dt} = \dot{E}_{\mathrm{h,HE,in}}(T_{\mathrm{h,HE,in}}) - \dot{E}_{\mathrm{h,HE,out}}(T_{\mathrm{h,HE,out}}) - U_{\mathrm{HE}}\cdot A_{\mathrm{HE}}\cdot(T_{\mathrm{h,HE}} - T_{\mathrm{c,HE}}) \tag{7}$$

$$\text{cold fluid}: \quad C_{\mathrm{c}}\frac{dT_{\mathrm{c,HE}}}{dt} = \dot{E}_{\mathrm{c,HE,in}}(T_{\mathrm{h,HE,in}}) - \dot{E}_{\mathrm{c,HE,out}}(T_{\mathrm{c,HE,out}}) + U_{\mathrm{HE}}\cdot A_{\mathrm{HE}}\cdot(T_{\mathrm{h,HE}} - T_{\mathrm{c,HE}}) \tag{8}$$

Further details on the extension of Eqs. (7) and (8) to the pre-reformer can be found in [20].

3. Low-level control requirements in SOFC systems

Once the design phase of an SOFC system is fulfilled, the following step is to develop suitable control strategies aimed at meeting

electrical load requirements while guaranteeing safe operation of ceramic components with respect to thermal stress issues. The former goal is obtained by properly selecting actual operating current as function of power demand. In case of pressurized systems [18], such a goal can be pursued also aiming at letting the SOFC system operate at maximum efficiency, which in turn results, as it happens for all fuel cell typologies [27–29], in determining the optimal trade-off between pressure and load increase. The latter goal (i.e. safe operation) can be achieved by setting-up a proper thermal management strategy. Indeed, outlet temperature control is one of the key requirements for SOFC stacks, especially if operated in transient conditions such as in transportation applications [30]. This is due to the severe thermal stresses imposed on cell materials by temperature variation subsequent to load change. Previous studies [3,13] indicated that in planar designs temperature increase across the cell should not overcome 100–150 °C to ensure the cell component's integrity. To meet such a requirement, the variable to be managed is the excess of air, which can be suitably regulated acting on the drive motor of the air compressor (see Fig. 2).

Moreover, two further issues must be certainly taken into account: (i) the need of limiting temperature derivatives during system warm-up; (ii) SOFC stack does not deliver any power until its operating temperature is lower than 700 °C [31]. Therefore, two separate control problems must be faced, the first aimed at fulfilling load demand at warmed-up (i.e. regime) conditions, the second concerning proper thermal management of the SOFC stack during cold-start phases.

Before reporting the description of warmed-up and start-up control strategies, an explanation of how the controlling hardware allows achieving the two tasks is given hereafter. With reference to Fig. 2, by acting on the four valves (V1–V4) the two main streams entering the stack (air and fuel) are controlled to attain the stack thermal targets: temperature time-derivative and temperature gradient. Therefore, the hardware must guarantee that both gases have fixed inlet stack temperature (700 °C) and proper flow rates, ensuring the right heating/cooling of the stack to reach the desired outlet temperature of 825 °C. It is worth reminding that when the current is drawn from the stack the outlet temperature also depends upon the electrochemical reaction occurring inside the stack. The anode inlet temperature depends upon the pre-reforming process whose temperature control is achieved by acting on the by-pass valve V3, which modulates the hot exhaust gases from the post burner. When no current is drawn (i.e. during warm-up), valves V1 and V2 deviate the fuel towards the post-burner and the valve V3 is closed. Valve 4 regulates the exhaust gases flowing into the pre-heater to guarantee heat-up of the air. To obtain a good control of stack temperature valve 4 management is coupled with the air compressor strategy. In the following sections a detailed description of the two control strategies is given.

4. Low-level control in warmed-up conditions

Fig. 3 describes the low-level control logic adopted for optimal management of warmed-up (WU) SOFC system. The reader is addressed to Fig. 2 for the physical plant layout. In Fig. 3 both stack input and output variables are reported together with the main controlling devices (i.e. valves and compressor). For SOFC, which exhibits a slow thermal dynamics, a feedback control based on the measured stack outlet temperature may not guarantee a proper thermal management; therefore a combination of feedforward and feedback controllers was implemented to achieve a precise thermal management of the stack. The feedback control logic is applied to the air compressor through a proportional integral PI controller to feed the excess air needed to keep outlet temperature at the desired value. On the other hand the feedforward strategy controls

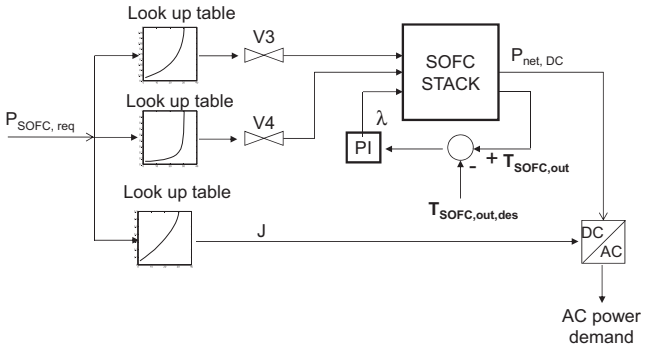

Fig. 3. Low-level control logic at regime conditions (i.e. WU) for the SOFC system illustrated in Fig. 2.

the DC/AC inverter and the valves V3 and V4. Three look-up tables estimate, as function of power requested from the stack, the current load and position of the by-pass valves V3 and V4 (see Fig. 2). It is worth reminding that during WU conditions the valve V1 is closed and valve V2 is kept fully open. In the following subsections the details about low-level rules definition and their impact on the dynamic behavior of SOFC systems are presented and discussed.

4.1. Temperature control

Fig. 3 also schematizes the PI control architecture developed to limit temperature gradient across the planar co-flow SOFC stack. The control action is obtained regulating the amount of air fed by the compressor by properly acting on its drive motor (see Fig. 2). Optimal PI parameters were found seeking for the best dynamic performance of the controller [20]. Fig. 4 shows the comparison between un-regulated and regulated compressor operation under a step variation in current density from 0.4 up to 0.7 A cm^{-2}. As expected, the PI controller reacts by increasing the excess of air (see Fig. 4c), thus limiting both duration of voltage undershoot and outlet temperature increase subsequent to the load step, as shown in Fig. 4a and b.

4.2. Heat exchanger control

In order to ensure that both cathode and anode inlet temperatures set to their operating values, the valves V3 and V4 shown in Fig. 2 must be suitably regulated with respect to the nominal working condition (i.e. 0.8 A cm^{-2}). At the design point the valves are fully closed and the whole mass flow rate of hot gases, coming from the post-burner, pass through both the pre-reformer and the air pre-heater, i.e. no by-pass takes place. In the current work, feed-forward valve control laws were obtained by imposing that both air and fuel reformate enters the stack at 700 °C. The following optimization procedure was adopted to find V3 and V4 control laws:

$$\min_{V_i} \Delta T_y(V_i, J) \quad i = [3, 4]; \tag{9}$$

$$\Delta T_y = \left| T_{y,out} - 700 \right|, \quad y = [\text{air pre-heater, pre-reformer}] \tag{10}$$

Fig. 5 reports the optimal fractions of fluid that by-pass the pre-reformer (a) and the air pre-heater (b) as function of the net required power. As expected, at low loads both valves are open, thus the minimum flow rate of hot gases is used to heat up anodic and cathode gases; this avoids overheating the lower fuel and air mass flows as compared to the nominal working point. The comparison between V3 and V4 values indicates a request of less heat for fuel reforming and warming-up of the anodic gases than that required at the cathode side. Therefore an almost fully open V3 is obtained from the optimization (see Eq. (9)) for a wide range of loads. On

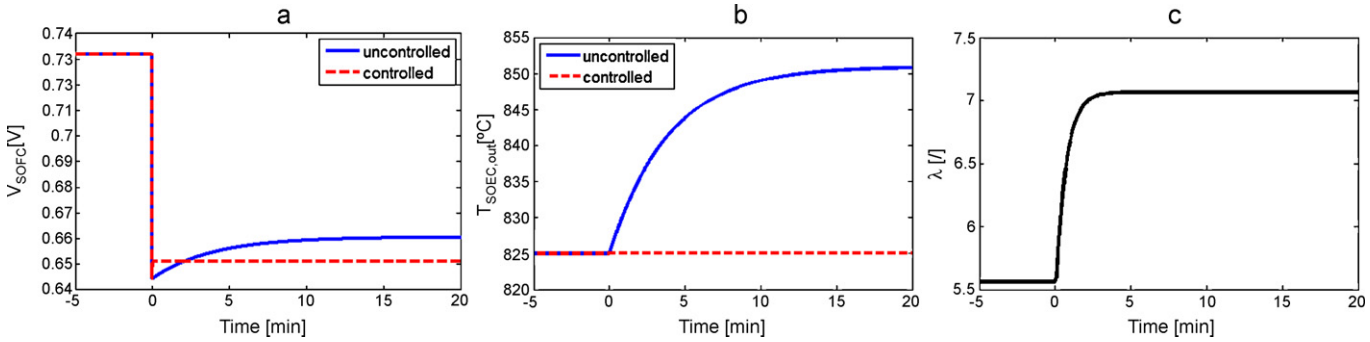

Fig. 4. (a) Comparison between controlled and uncontrolled voltage response to a step change in current density; (b) comparison between controlled and uncontrolled temperature response to a step change in current density; (c) action on excess of air exerted by the WU PI controller.

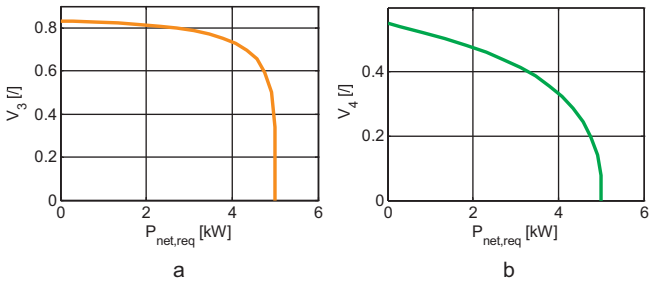

Fig. 5. Control maps for determining optimal heat exchanger valve position as function of power demand, pre-reformer by-pass valve (a) and air pre-heater (b).

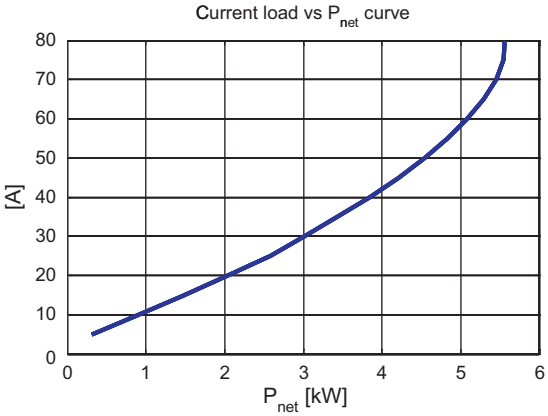

Fig. 6. Performance curve for the SOFC unit design described in Fig. 2.

the other hand the valve V4 needs to be regulated carefully, this is expected since the air has a critical role due to its cooling action on the stack. Furthermore, the heat exchange between exhausts and fresh air has not to be reduced too much in the air pre-heater since the cathode flow is larger than the anodic one, thus imposing a reduced by-pass flow, as shown in Fig. 5b.

4.3. Load following strategy

Current to be drawn from the stack to meet actual power demand is found via the performance curve shown in Fig. 6, which was developed by means of the SOFC system model presented in Section 2.1. The low-level component through which load-following is enabled is a switching converter, to be placed at system output before the conversion from DC to AC (see Fig. 2). Particularly, proper action [32] on the converter duty cycle allows modifying the equivalent resistance upstream of the converter in such a way as to let the SOFC system work at the desired load, as addressed by the map shown in Fig. 6.

Once the warmed-up control strategies development is accomplished, it is possible to simulate, by the model expressed by Eqs. (1)–(8) the SOFC system dynamic response to load change. Fig. 7 shows voltage and ΔT response to a step variation from $P_{net,0} = 1.9$ kW up to two values of $P_{net,f}$ (2.7 and 5 kW). In Fig. 7b ΔT denotes the flow temperature difference across the cathode; it is worth noting that in the lumped approach the cathode outlet temperature corresponds to the stack temperature, thus $\Delta T = T_{SOFC,out} - T_{cat,in}$. As expected (see Section 4.1) V_{SOFC} exhibits an undershoot-response to load increase, while ΔT responds with an overshoot depending on the difference $P_{net,f} - P_{net,0}$. In both

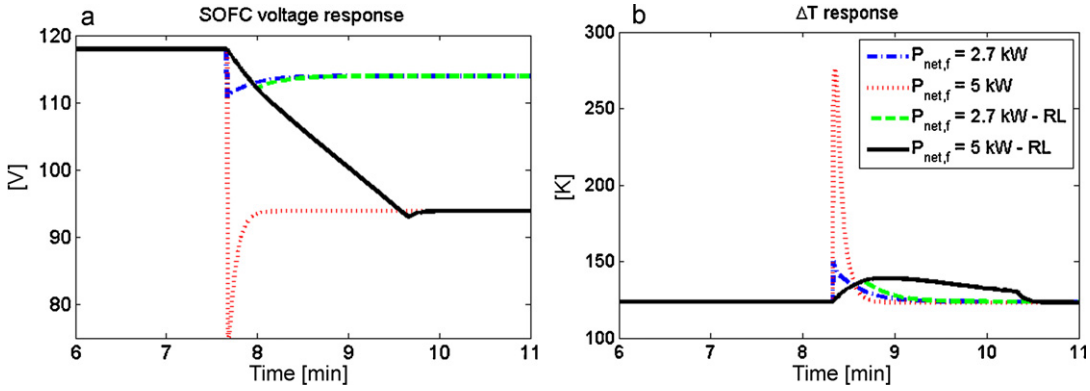

Fig. 7. Impact of rate limiter on dynamic SOFC response under load transient, with voltage excursion on plot (a) and temperature difference across the cathode flow on plot (b). The (b) legend applies for both figures.

Table 1
Synthesis of valves control logic during system warm-up. The symbols v and k stand for "varying" and "constant", respectively. The following phases are described: cold-start (CS); power supply (PS – i.e. current start to be drawn during warm up); transition from CS to WU (CS–WU); warmed-up (WU).

		V1	V2	V3	V4	λ	CH_4
1	CS	1	0	1	0	v	k
2	PS	v	v	v	0	v	k
3	CS–WU	0	1	v	v	v	k
4	WU	0	1	v	v	v	v

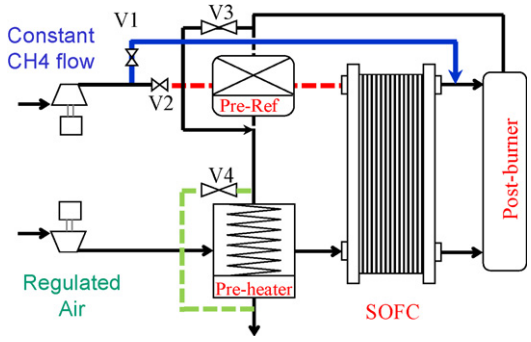

Fig. 8. Cold-start management of main SOFC system actuators. Dotted lines refer to closed pipes.

the analyzed cases, ΔT overshoot is significantly high, thus potentially causing damaging thermal stresses along the gas channels [8]. In order to avoid such a dangerous behavior during transient operation of the SOFC unit, a rate limiter (RL) on requested P_{net} must be introduced. This way, the SOFC system will dynamically

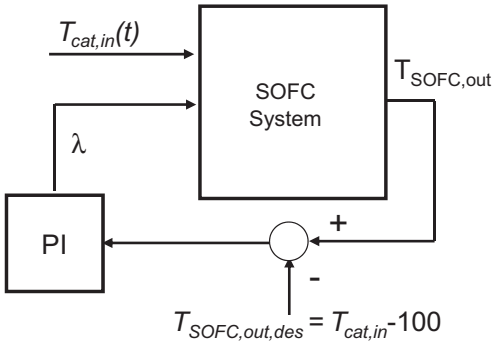

Fig. 9. Logic of the PI controller to be implemented for proper cold-start control of excess of air (λ).

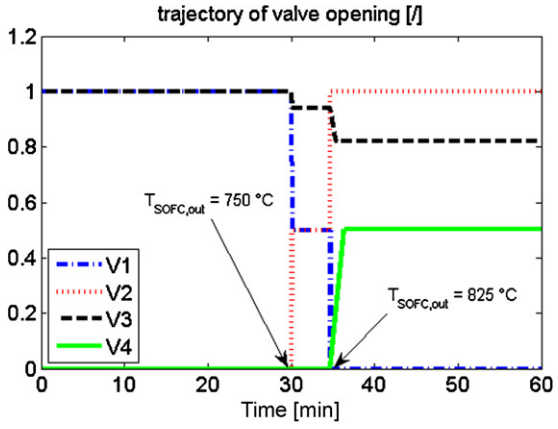

Fig. 10. Description of valves trajectory during cold-start time history (see Table 1).

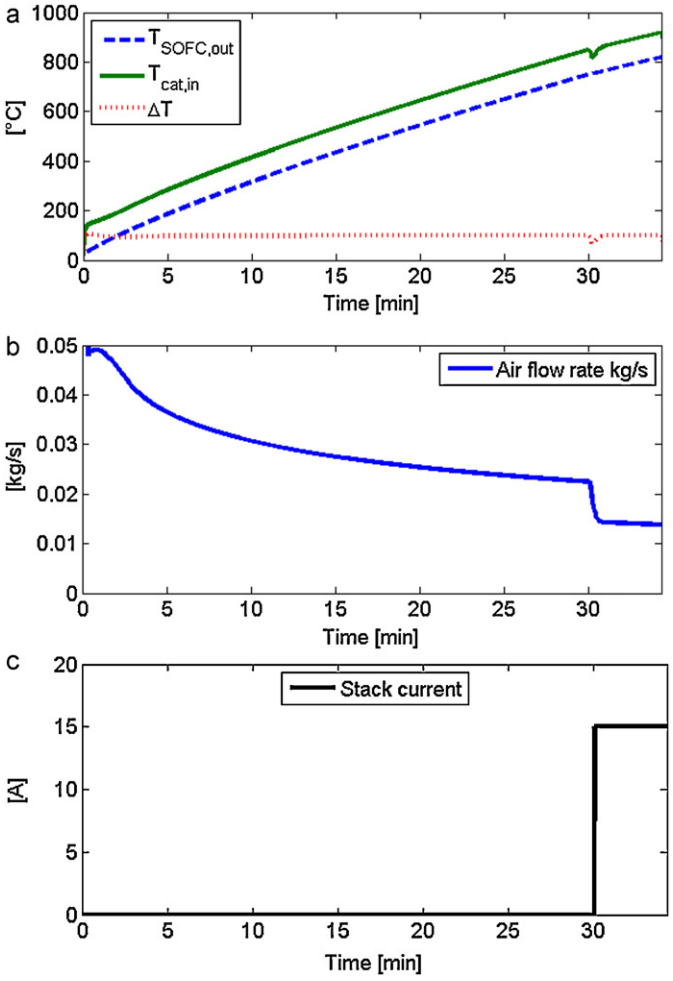

Fig. 11. Temperatures variation (a), trajectory of the controlled variable (b) and load (c) during phase cold start (CS).

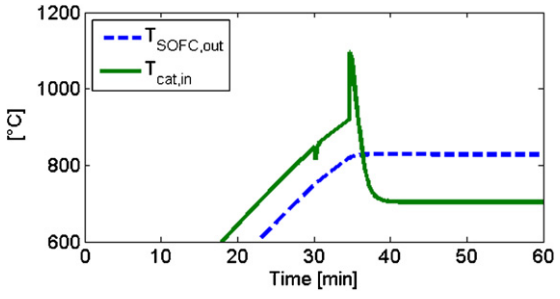

Fig. 12. Close window showing the detrimental effect of threshold base transition CS–WU.

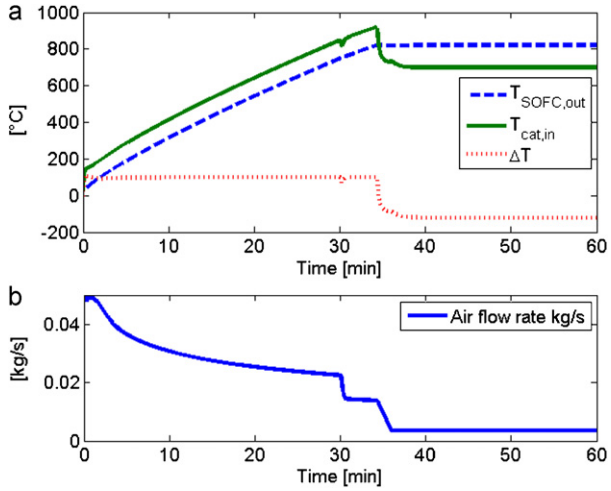

Fig. 13. Temperatures variation (a) and trajectories of controlled variables during the entire warming-up process (i.e. from phase 1 to phase 4, see Table 1).

respond to ramp load variation. Fig. 7 shows that a rate limiter with RL = 0.03 kW s^{-1} allows limiting ΔT variations within a safe bound (i.e. 20 K). Of course, the adoption of a rate limiter would require an energy buffer, such as a battery pack, to cope with the difference between requested power and SOFC power supply during transients.

5. Low-level control during SOFC start-up

The start-up strategy proposed in this work is divided into three main phases to guarantee a safe transition from zero load at ambient temperature to warmed up conditions (see previous section). The start-up presented herein refers to the maneuver of an APU and represents the most critical operation for an SOFC due to the reduced time requested to achieve the full load state and the possible number of start-up occurring in e.g. automotive applications [20].

During SOFC cold-start (CS), ensuring integrity of the heterogeneous stack materials [33] entails limiting not only temperature gradient across the cell channels, but also stack temperature derivative. The first objective in cold start, which is common to warmed-up conditions, is achieved by properly acting on the mass flow of the heating fluid. In this work, stack heating is obtained by

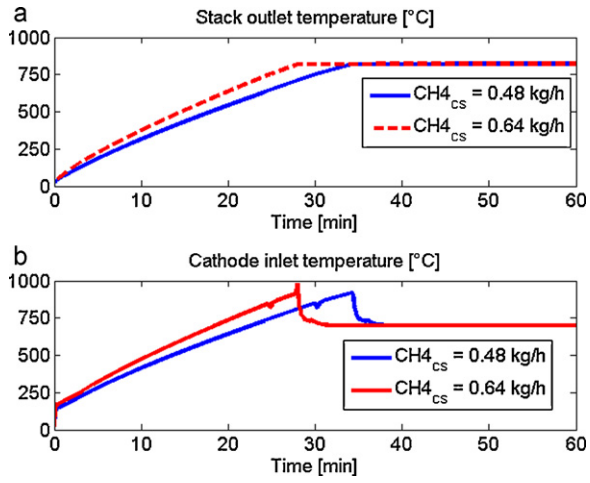

Fig. 14. Temperature variation of SOFC outlet (a) and cathode inlet (b) for different constant methane flow during CS phase (see Table 1).

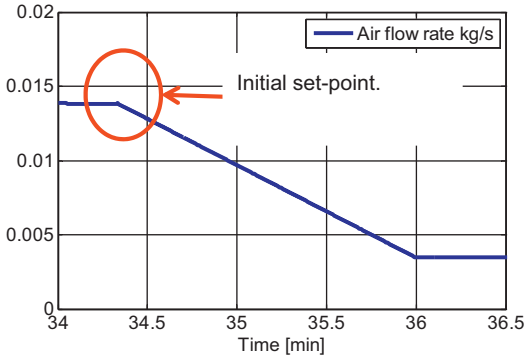

Fig. 15. Linear reduction of air flow in the transition CS–WU.

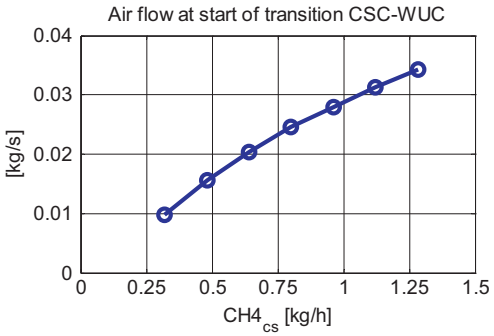

Fig. 16. Dependence of optimal $\dot{m}_{air,in,cs-wu}$ on $\dot{m}_{CH_4,cs}$.

acting on valves V1 and V2 in order to by-pass the anode channels and, thus, directly supply methane to the post-burner, as shown in Fig. 8. In the post-burner, the methane reacts with the air coming out of the cathode channels, thus releasing the heat that will then be transferred to the incoming air fed by the compressor. Thus, the stack gets internally heated by the air flowing through the cathode channels, as it is usually required for SOFC technology [34].

The incoming air flow is the control variable to be managed to ensure that temperature gradient is safely limited under 100 °C [16], as shown in the control scheme depicted in Fig. 9. On the other hand, the methane flow is kept constant till the end of cold-start. It is worth remarking here that temperature increase across the stack in cold-start phase is $\Delta T_{cs} = -\Delta T$. In this study the small amount of reformate gas flowing through the anode to "prepare" the reaction was not considered since it does not affect the entire thermal balance.

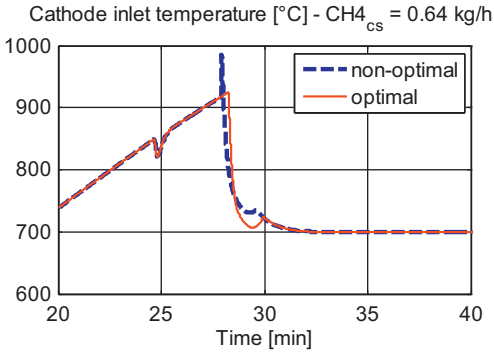

Fig. 17. Close window highlighting the importance of correctly setting the value of $\dot{m}_{air,in,cs-wu}$ to avoid dangerous temperature spike at cathode inlet.

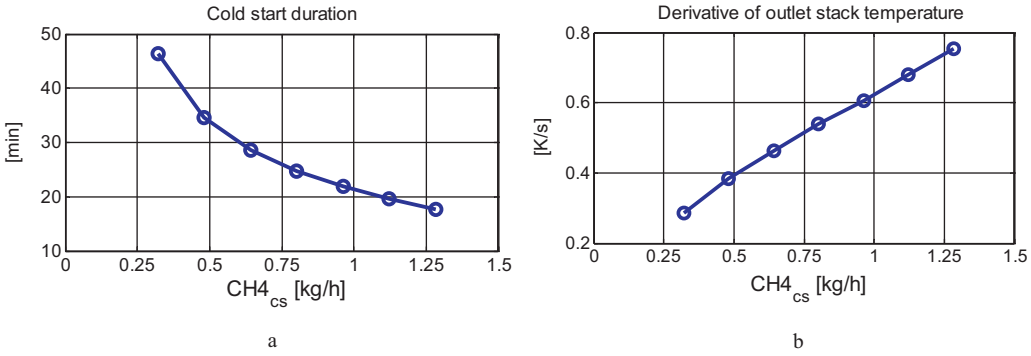

a b

Fig. 18. Dependence of cold-start duration (a) and stack temperature derivative on $\dot{m}_{CH_4,cs}$.

Since no current can be drawn until stack temperature is lower than 700 °C, it was assumed that no load is applied before $T_{SOFC,out}$ reaches 750 °C; this means that the bulk temperature is safely higher than 700 °C whenever current is drawn out of the stack. Once such condition is reached, a second phase starts (i.e. power supply – PS), which requires a different management of valves V1, V2, V3 and V4 (see Fig. 8). Table 1 and Fig. 10 summarize the valve scheduling to be followed to properly link cold-start to warmed-up operation in an SOFC system. When the second phase (i.e. PS in Table 1, $T_{SOFC,out} > 750$ °C) starts, V1 and V2 are half-open in order to split the methane flow between pre-reformer and post-burner. Therefore, in order to enable external reforming, V3 is partially closed to allow post-burner exhausts to deliver some heat to the pre-reformer. Then, before entering the warmed-up strategy (i.e. phase WU), proper transition (i.e. phase CS–WU) of valves aperture has to be performed as discussed in the next subsection.

5.1. Temperature control during cold-start

Fig. 11 shows the performance of the cold-start PI controller sketched in Fig. 9 during phase CS (see Table 1). Particularly, in Fig. 11a it can be seen how such controller is always capable of keeping ΔT_{cs} at 100 °C till the PS phase starts (approximately after 30 min as shown in Fig. 11c). At this point, a small variation of ΔT_{cs} occurs due to the current drawn from the stack, which in turn causes direct methane flow to the post-burner to be reduced. Therefore, a lower amount of air has to be fed by the air compressor to avoid overcooling the stack (see Fig. 11b). Then, after 34 min, $T_{SOFC,out}$ finally reaches its set-point value, thus requiring switching from cold-start to warmed-up temperature control strategy. Nevertheless, a threshold base instant switching results in a highly detrimental increase in cathode inlet temperature, as shown in Fig. 12. Therefore, proper transition strategy from CS to WU is needed. In this study the CS–WU phase consists of a linear reduction of excess of air down to the WU set-point, as shown in the time window 35–37 min of Fig. 13b. The comparison of Fig. 12 and Fig. 13a evidences how such an approach allows to fully remove the undesired inlet cathode temperature spike, thus ensuring stack integrity be preserved.

5.2. Influence of methane set-point variation on cold-start performance

In some applications, such as SOFC systems designed and developed as Auxiliary Power Units for automotive use, a satisfactory compromise between rapid cold-start and thermal stress issues must be found. Focusing on the control strategy presented in the above paragraphs, the variable to be managed to perform such trade-off analysis is the constant methane flow fed in the CS and PS phases (see Table 1). Fig. 14a shows that increasing the methane flow (i.e. $\dot{m}_{CH_4,cs}$), as compared to the base value considered in Section 5.1 (i.e. $\dot{m}_{CH_4,cs} = 0.48$ kg/h) results in a quicker CS phase. Nevertheless, such a different approach entails properly identifying the initial set-point of the linear reduction of air-flow (i.e., $\dot{m}_{air,in,cs-wu}$ see Fig. 15). Indeed, if $\dot{m}_{air,in,cs-wu}$ is not varied as function of $\dot{m}_{CH_4,cs}$ a spike in cathode inlet temperature occurs when the CS–WU phase starts, as shown in Fig. 14b. Therefore, the SOFC simulator described in Section 2.1 can be profitably utilized to identify the dependence of optimal $\dot{m}_{air,in,cs-wu}$ on $\dot{m}_{CH_4,cs}$ as shown in Fig. 16. Fig. 17 confirms the validity of such an approach to remove the aforementioned temperature spike in cathode inlet at the beginning of the CS–WU phase.

Finally, Fig. 18 shows the variation of SOFC start-up time and $T_{SOFC,out}$ derivative as function of $\dot{m}_{CH_4,cs}$. It can be seen that imposing low temperature derivatives (i.e. in the range [0.3–0.5], which can be considered reasonably safe [35]) requires prolonging SOFC start-up up to 45 min (see Fig. 18a). On the other hand, faster cold-start may result in too high derivatives, of the order of 0.8 K s^{-1}, as shown in Fig. 18b. Therefore, the model-based evaluation of start-up time dependence on methane mass flow fed to the post-burner is well suited to solve the trade-off between rapid cold-start and thermal stress depending on the specific application field to which the SOFC system is destined.

6. Conclusions

In the paper control-oriented modeling methodologies were proposed to develop specific strategies aiming at ensuring proper energy management of SOFC systems. The hierarchical modeling approach that was adopted to meet the conflicting needs of high accuracy, acceptable experimental burden and low computational intensity was presented and motivated. Then, the main requirements for optimal low-level control of SOFC systems were recalled and discussed to guarantee the best compromise between efficient use and safe operation of SOFC stacks. Moreover, significant attention was devoted to identify the main actuators to be considered when developing effective control laws.

Model-based design of low-level control strategies was performed to address not only the separate definition of warmed-up and cold start management strategies for SOFC system, but also to guarantee proper transition between such phases.

The SOFC simulator was shown to be useful to find the best trade-off between rapid cold-start and thermal stress issues. Future work will focus on BoP sub-models improvement (e.g. actuators dynamics) and the development of monitoring and diagnostics strategies for appropriate management of SOFC systems in both transient and stationary operations.

References

[1] Solid State Energy Conversion Alliance (SECA), 2010, reachable in October 2010 at http://www.netl.doe.gov/technologies/coalpower/fuelcells/seca/.
[2] S.C. Singhal, Solid State Ionics 152–153 (2002) 405–410.
[3] R.J. Braun, Optimal design and operation of solid oxide fuel cell systems for small-scale stationary applications, Ph.D. Thesis, University of Wisconsin, Madison, WI, 2002.
[4] European Fuel Cell and Hydrogen Joint Technology Initiative, 2009. Available from: <https://www.hfpeurope.org/hfp/jti>.
[5] T. Ujiie, 207th ECS Meeting, MA2005-01, May 15–May 20, 2005, Quebec City, Canada, 2006.
[6] Topsoe, Topsoe Fuel Cell and Wärtsilä Corporation demonstrate operating results, 2006. Available from: <http://www.topsoe.com/News/ PressReleases/2006.aspx>.
[7] R. Rosenberg, European SOFC Stakeholders Workshop, November 26–27, Sofia, Bulgaria, 2008.
[8] P. Aguiar, C.S. Adjiman, N.P. Brandon, J. Power Sources 138 (2004) 120–136.
[9] L.A. Chick, R.E. Williford, J.W. Stevenson, C.F. Windisch Jr., S.P. Simner, Proceedings of Fuel Cell Seminar, PNNL-SA-37014, 19–21 November, 2002, Palm Springs, CA, 2002.
[10] M. Iwata, T. Hikosaka, M. Morita, T. Iwanari, K. Ito, K. Onda, Y. Esaki, Y. Sakaki, S. Nagata, Solid State Ionics 132 (2000) 297–308.
[11] D. Bhattacharyya, R. Rengaswamy, Ind. Eng. Chem. Res. 48 (2009) 6068–6086.
[12] E. Achenbach, J. Power Sources 57 (1995) 283–288.
[13] P. Aguiar, C.S. Adjiman, N.P. Brandon, J. Power Sources 147 (2005) 136–147.
[14] K. Sedghisigarchi, A. Feliachi, IEEE Trans. Energy Conver. 2 (19) (2004) 423–428.
[15] K. Sedghisigarchi, A. Feliachi, IEEE Trans. Energy Conver. 19 (2) (2004) 429–434.
[16] N. Lu, Q. Li, X. Sun, M.A. Khaleel, J. Power Sources 161 (2006) 938–948.
[17] P.H. Lin, C.W. Hong, J. Power Sources 187 (2009) 517–526.
[18] M. Sorrentino, A.Y. Mandourah, T.F. Petersen, Y.G. Guezennec, M.J. Moran, G. Rizzoni, Proceedings of the 2004 ASME IMECE, November 13–19, 2004, Anaheim, California, USA, 2004.
[19] M. Sorrentino, C. Pianese, Y.G. Guezennec, J. Power Sources 180 (2008) 380–392.
[20] M. Sorrentino, C. Pianese, J. Fuel Cell Sci. Technol. 6 (2009), 041011/1–041011/12.
[21] M. Sorrentino, C. Pianese, Proceedings of the European Fuel Cell Forum 2009, Lucerne, Switzerland, June 29–July 2, 2009.
[22] G. Rizzoni, J.R. Josephson, A. Soliman, C. Hubert, C.G. Cantemir, N. Dembski, P. Pisu, D. Mikesell, L. Serrao, J. Russell, M. Carroll, in: Proceedings of the SPIE, J. Unmanned Ground Veh. Technol. VII 5805 (2005) 1–12.
[23] I. Arsie, A. Di Domenico, C. Pianese, M. Sorrentino, in: ASME Transactions, J. Fuel Cell Sci. Technol. 4 (2007) 261–271.
[24] D. Hissel, M.C. Péra, J.M. Kauffmann, J. Power Sources 128 (2) (2004) 239–246.
[25] M.J. Moran, H.N. Shapiro, Fundamentals of Engineering Thermodynamics, John Wiley and Sons, Hoboken, NJ (USA), 2004, pp. 681–683.
[26] O.E. Ataer, A. Ileri, Y. Gogus, Int. J. Refrig. 18 (3) (1995) 153–160.
[27] J.T. Pukrushpan, A.G. Stefanopoulou, H. Peng, Proceedings of the American Control Conference, Anchorage, AK, 2002, pp. 3117–3122.
[28] J. Reuter, U.J. Beister, N. Liu, D. Reuter, B. Eybergen, M. Radhamohan, A. Hutchenreuther, Control of a fuel cell air supply module (ASM), SAE Paper No. 2004-01-1009, 2004.
[29] A. Di Domenico, A. Miotti, M. Alhetairshi, Y.G. Guezennec, S. Rajagopalan, S. Yurkovich, in: Proceedings of the American Control Conference, Minneapolis, MN, Jun. 14–16 (2006).
[30] J.J. Botti, M.J. Grieve, J.A. MacBain, Electric vehicle range extension using an SOFC APU, SAE Paper No. 2005-01-1172, 2005.
[31] A. Weber, E.I. Tiffée, J. Power Sources 127 (2004) 273–283.
[32] A. Giustiniani, G. Petrone, G. Spagnuolo, I. Arsie, A. Di Domenico, C. Pianese, M. Sorrentino, M. Vitelli, in: ASME Transactions, J. Fuel Cell Sci. Technol. 7 (2010) 011021/1–011021/11.
[33] R.M. Ormerod, Chem. Soc. Rev. 32 (2003) 17–28.
[34] H. Apfel, M. Rzepka, H. Tu, U. Stimming, Journal of Power Sources 154 (2006) 370–378.
[35] M.L. Ferrari, A. Traverso, L. Magistri, A.F. Massardo, J. Power Sources 149 (2005) 22–32.